

Inner solar system material discovered in the Oort cloud

Karen J. Meech,^{1*} Bin Yang,² Jan Kleyna,¹ Olivier R. Hainaut,³ Svetlana Berdyugina,^{1,4} Jacqueline V. Keane,¹ Marco Micheli,^{5,6,7} Alessandro Morbidelli,⁸ Richard J. Wainscoat¹

2016 © The Authors, some rights reserved; exclusive licensee American Association for the Advancement of Science. Distributed under a Creative Commons Attribution NonCommercial License 4.0 (CC BY-NC). 10.1126/sciadv.1600038

We have observed C/2014 S3 (PANSTARRS), a recently discovered object on a cometary orbit coming from the Oort cloud that is physically similar to an inner main belt rocky S-type asteroid. Recent dynamical models successfully reproduce the key characteristics of our current solar system; some of these models require significant migration of the giant planets, whereas others do not. These models provide different predictions on the presence of rocky material expelled from the inner solar system in the Oort cloud. C/2014 S3 could be the key to verifying these predictions of the migration-based dynamical models. Furthermore, this object displays a very faint, weak level of comet-like activity, five to six orders of magnitude less than that of typical ice-rich comets on similar orbits coming from the Oort cloud. For the nearly tailless appearance, we are calling C/2014 S3 a Manx object. Various arguments convince us that this activity is produced by sublimation of volatile ice, that is, normal cometary activity. The activity implies that C/2014 S3 has retained a tiny fraction of the water that is expected to be present at its formation distance in the inner solar system. We may be looking at fresh inner solar system Earth-forming material that was ejected from the inner solar system and preserved for billions of years in the Oort cloud.

INTRODUCTION

Small primitive bodies were witness to the solar system's formative processes. When gas was present in our solar system's protoplanetary disk, during the first 5 million years of solar system formation, a local chemical signature was imprinted on the planetesimals. The connection to today's solar system relies on how this material was dynamically redistributed during the planet-forming process. To connect early planet formation to the modern era, we must measure the compositions of a range of primitive bodies from different locations in the solar system and compare them with the predictions from models of early solar system formation, some of which predict significant reshuffling of material throughout the solar system. Ground- and space-based observations of comets have played a key role in mapping out early solar system chemistry, and observations of protoplanetary disks are now generating chemical maps of other forming planetary systems for use as constraints of disk chemical models.

Currently, several dynamical models can reproduce much of our solar system's current architecture. The "Grand Tack" model (1) starts the simulation of solar system formation at an early phase, when the giant planets grew and migrated in a gas-rich protoplanetary disk. During their inward migration, the giant planets scattered inner solar system material outward; during their outward migration, they implanted a significant amount of icy planetesimals [from 3.5 to 13 astronomical units (AU)] into the inner solar system. The Grand Tack

model predicts the presence of rocky objects in the Oort cloud at an icy comets/rocky asteroids ratio of 500:1 to 1000:1 (see section S1 for an expanded discussion of the dynamical models and their predictions). Other dynamical models, which assume nonmigrating giant planets, make different predictions about the fraction of the Oort cloud population comprising planetesimals initially within the asteroid belt or the terrestrial planet region. These predictions range from 200:1 to 2000:1 (2, 3). Other models do not explicitly estimate the mass of rocky planetesimals eventually implanted in the Oort cloud (4), but from the amount initially available, it is reasonable to expect that the ratio of icy planetesimals to rocky planetesimals in the final Oort cloud is between 200:1 to 400:1. Instead, a recent radically different model of terrestrial planet formation predicts that the planetesimals in the inner solar system always had a negligible total mass (5); in this case, there would be virtually no rocky Oort cloud population.

RESULTS

As described in Section "Materials and Methods" C/2014 S3 (PANSTARRS) has an orbit typical of that of a returning Oort cloud comet. Our analysis of the activity of C/2014 S3 suggests that dust coma is consistent with sublimation. The level of activity is five to six orders of magnitude lower than that of active long-period comets at a similar distance. The spectrum of C/2014 S3 is consistent with S-type asteroidal material, and the location and depth of the 1- μm band suggest that the material may be minimally thermally processed. This presents the intriguing possibility that we are seeing relatively fresh inner solar system material that has been stored in the Oort cloud and is now making its way into the inner solar system. The discovery and characterization of a rocky object from the Oort cloud is therefore the first step toward measuring the fraction of rocky objects in the Oort cloud. This will provide strong constraints for the models.

¹Institute for Astronomy, University of Hawai'i, 2680 Woodlawn Drive, Honolulu, HI 96822–1839, USA. ²European Southern Observatory, Alonso de Córdova 3107, Vitacura, Casilla 19001, Santiago, Chile. ³European Southern Observatory, Karl-Schwarzschild-Strasse 2, 85748 Garching bei München, Germany. ⁴Kiepenheuer Institut fuer Sonnenphysik, Schoeneckstrasse 6, 79104 Freiburg, Germany. ⁵Space Situational Awareness (SSA)–Near Earth Objects (NEO) Coordination Centre, European Space Agency, 00044 Frascati (RM), Italy. ⁶SpaceDyS s.r.l., 56023 Cascina (PI), Italy. ⁷Istituto Nazionale di Astrofisica (INAF)–Istituto di Astrofisica e Planetologia Spaziali (IAPS), 00133 Roma (RM), Italy. ⁸Laboratoire Lagrange, UMR 7293, Université de Nice Sophia-Antipolis, CNRS, Observatoire de la Côte d'Azur, Boulevard de l'Observatoire, 06304 Nice Cedex 4, France.

*Corresponding author. Email: meech@ifa.hawaii.edu

DISCUSSION

What are the implications of an active S-type object from the Oort cloud?

When Jan Oort (6) formulated his model of the Oort cloud, he inferred that too few comets were on their return passage through the solar system. He proposed that the comets faded as a result of physical evolution and volatile loss. However, it is expected that volatiles in ice-rich bodies should be able to sustain cometary activity for up to 1000 perihelion passages (3). Furthermore, models for the number of Oort cloud comets that enter the inner solar system and subsequently fade predict a large number of dormant isotropic long-period comets that are not seen (7). Thus, most Oort cloud comets must be lost because they physically disrupt, not because they become inactive because of volatile loss. Nevertheless, it cannot be excluded that some comets become inactive. The point is that inactive comets should have a D- or P-type spectrum, not an S-type reflectivity (8). Accordingly, we can conclude that C/2014 S3 is not an almost-extinct comet.

C/2014 S3 is not the first nearly inactive object on a long-period comet orbit to be found. The first, discovered by the Near-Earth Asteroid Tracking (NEAT) search, was 1996 PW (9). 1996 PW generated only moderate attention observationally, with observations indicating that it was not active, was red, had a radius of between 4 and 8 km, and was a slow rotator. An exploration of the dynamical history of 1996 PW to assess whether it was an extinct Oort cloud comet, an Oort cloud asteroid, or something more recently ejected outward, such as an extinct ecliptic comet or a main belt asteroid, showed that it was equally probable that 1996 PW was an extinct comet or an asteroid ejected into the Oort cloud during the early evolution of the solar system (3). More recently, other Manx candidates have been discovered. We have observed five of them, which also show comet-like red colors similar to 1996 PW. C/2014 S3 is the first and only Manx candidate to date with an S-type reflectivity spectrum.

What are the implications of seeing a low-level potentially volatile-driven activity from an object with an S-type spectrum on a returning long-period comet from the Oort cloud? Widespread evidence indicates aqueous alteration throughout primitive asteroids originating in the outer asteroid belt (10, 11). Evidence also suggests that water may still be present in the outer asteroid main belt—observable as outgassing from main belt comets (12) and dwarf planets (13) or as ice on the surfaces of asteroids (14).

S-type asteroids, which are dominant in the inner main asteroid belt today and formed from inner solar system material, are clearly inactive and are neither expected nor observed to have ice (15). Cosmochemical studies of meteorites have shown that many classes of meteorites underwent extensive aqueous processing in their parent bodies. The hydrated C- and D-type asteroids are commonly associated with carbonaceous chondrite meteorites (16), but the best match between meteorite classes and the S-type asteroids comes from the ordinary chondrites (OCs). This was confirmed with Hayabusa mission samples returned from the S-type asteroid Itokawa (17, 18).

The 1- μ m and 2- μ m absorption bands in the near-infrared (NIR) and the visible NIR spectral slope are used to interpret surface mineralogies of S-type asteroids. The relative band centers and depths can be used to assess the relative abundance of olivine-pyroxene and the Fe²⁺ and Ca²⁺ contents in these minerals. The spectral slope in the 1- to 2- μ m region is related to the FeNi metal content and olivine abundance (19). The wide range of S-type mineralogical variations have been

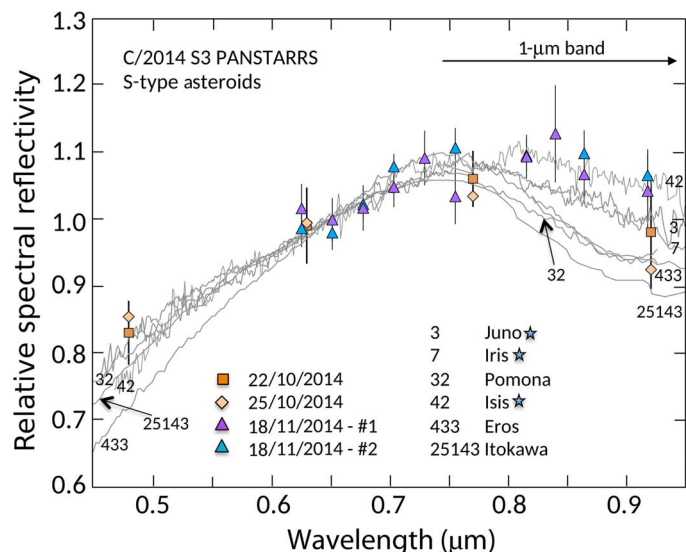


Fig. 1. CFHT photometry converted into spectral reflectivity obtained on UT (Universal Time) 22 and 25 October 2014, is shown in comparison to the VLT reflectivity spectrum obtained on UT 18 November 2014. Data beyond 0.9 μ m were affected by bright night sky emission lines that could not be subtracted satisfactorily; they are included for comparison with the CFHT data. Two independent methods were used to process the spectra (#1 and #2). The spectra have been binned to increase the signal-to-noise ratio. The location of the 1- μ m band characteristic of S-type asteroids is shown, and the spectra of six S-type asteroids with a shallow 1- μ m feature are shown for comparison (17, 32); the star symbols denote the S(IV)-type asteroids. All spectra are normalized to 0.65 μ m. The data for C/2014 S3 are consistent with these S-type asteroids.

divided into subclasses, with the S(IV) class matching C/2014 S3 best (Fig. 1). The S(IV) class most likely represents the parent bodies of the OC meteorites. The silicates (olivine and pyroxene) inferred for the S(IV) asteroids are similar to unequilibrated OCs (UOCs) (19). The UOCs are the most primitive of the OCs, never reaching very high temperatures (15). The UOCs have olivine/(olivine + low-calcium pyroxene) ratios, which are manifested in a very shallow 1- μ m band similar to that seen in (3) Juno and (7) Iris (20). The surface of C/2014 S3 appears to be consistent with more primitive S-type material.

Chondrite accretion ages and the conditions under which they were aqueously altered can be used to constrain where they accreted. Previously, because of the absence of carbonates in OCs and the lack of proper standards, there had been no reliable ages for aqueous activity for OC parent bodies. New work on an L3 chondrite (one of the most pristine OCs) has now shown the presence of fayalite, a secondary mineral that is a product of aqueous alteration (21). The mineralogy and thermodynamic analysis of the sample showed that the fayalite was consistent with formation at low temperatures and a low water/rock mass ratio (0.1–0.2)—much lower than measured values in comets (22). Accretion ages between 1.8 and 2.5 million years after the formation of the first solar system solids for the L-parent bodies, and the ages at which the aqueous secondary minerals formed, suggest that some water ice was incorporated into the accreting parent bodies and that they accreted close to the protoplanetary disk snowline (21). The snowline likely varied in position over time, but many models suggest that, toward the end of the protoplanetary disk phase, it could have been within the terrestrial planet-forming region (23). This is close

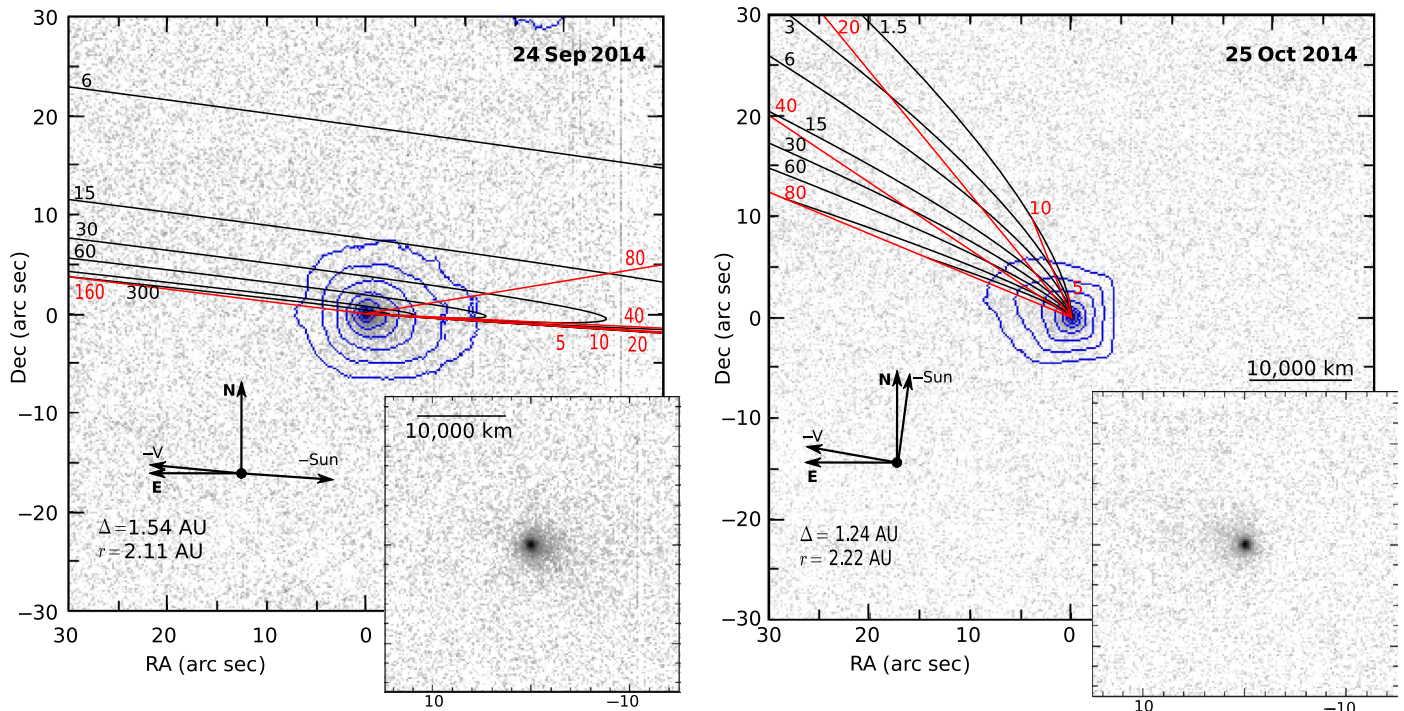


Fig. 2. Images of C/2014 S3 (PANSTARRS) obtained on 24 September 2014 (left) and 25 October 2014 (right) with the CFHT. The background stars have been processed out of these composites. The comet was at heliocentric distances (r) of 2.11 and 2.22 AU, moving outward from its perihelion at 2.05 AU on 13 August 2014. The syndynes (black; grain sizes are expressed in micrometers) and synchroes (red; positions noted in days before the observations) map out the expected position of the dust released from the nucleus under the influence of solar radiation pressure. Different lines indicate the locus of dust of different sizes released at different times; the marked change between the two epochs reflects very different viewing geometries. The blue isophotes are equally spaced on a logarithmic scale. The insets are at the same scale as the main images. The arrows indicate the directions of North and East and of the antisolar and negative of the heliocentric velocity vectors ($-V$). Dec, declination; RA, right ascension; Δ , geocentric distance.

to where the OC parent bodies were believed to be accreted. Although the minerals in the OCs are anhydrous and formed under dry conditions, it is possible that they could have acquired some water later.

These observations may tie together other reported observations that appeared to contradict the current understanding of solar system formation. There was clear evidence in the comet dust samples from the Stardust mission that there had been substantial radial migration in the protoplanetary disk, with comet dust having seen regions of high temperature (24). Fluid water inclusions have been found in the Monahans OC, and one possible explanation for this was that water was exogenously delivered after it formed (25). The Orgueil meteorite has long been considered a candidate for a possible cometary origin or from a body rich in volatiles (26). The discovery of C/2014 S3, an object on a cometary orbit that has the characteristics of an inner solar system asteroid, can offer new ideas about the relation between meteorites and their sources.

The discovery of C/2014 S3 on the orbit of an Oort cloud comet, made of minimally thermally processed rocky S-type material strongly suggests that this object is one of the interlopers predicted by the various dynamical evolution models of the early solar system. These models make predictions about the amount of inner solar system material that could reside in the Oort cloud as a result of scattering by the giant planets, and these predictions radically differ depending on the initial mass of the asteroid population that these models assume/imply. Assessing how many S-type objects exist will be a strong test of these

models. To unambiguously select between dynamical models, we need to characterize 50 to 100 Manx objects; the number of S-types found will distinguish between the models (see section S6 for a statistical assessment of the number of objects to be observed).

MATERIALS AND METHODS

On 22 September 2014, the Panoramic Survey Telescope and Rapid Response System (Pan-STARRS) telescope (PS1) discovered a weakly active comet at a heliocentric distance of 2.1 AU, designated C/2014 S3 (PANSTARRS) (hereafter, C/2014 S3). C/2014 S3 has a long-period comet orbit (semimajor axis, 90.5 AU; eccentricity, 0.977; perihelion, 2.049 AU; aphelion, 178.9 AU; inclination, 169.3°; period, 860.3 years) whose source reservoir is most likely the Oort cloud (27). Because of the nearly tailless appearance of the object at a distance where long-period comets are very active, the object has been called a “Manx” comet, after the tailless cat. Observations in the days after the discovery suggested that C/2014 S3’s colors might be interesting, so follow-up multifilter observations were obtained on 22 and 24 October 2014 using the Canada-France-Hawaii Telescope (CFHT), and spectra were acquired on 18 November 2014 using the Very Large Telescope (VLT) in Chile. Images of C/2014 S3 are shown in Fig. 2, and the reflectivity spectrum is shown in Fig. 1 (sections S2 and S3 provide details on the observations and data reduction).

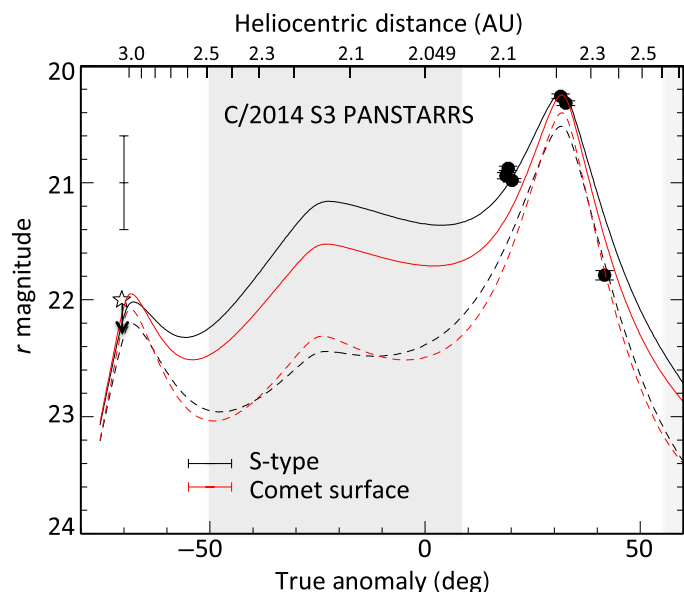


Fig. 3. Water ice sublimation models compared to measured *r*-band brightness as a function of position along the orbit [true anomaly (TA) = 0° is at perihelion]. The solid line shows the total brightness contribution from the nucleus and the dust, and the dashed line shows the contribution from the nucleus only. Models for a low-albedo comet nucleus surface and a brighter S-type asteroid surface are shown. By TA = 41.7°, the activity had significantly decreased. No combination of nucleus size and activity level can reproduce all the data without assuming a decrease in activity; the best fit is presented. The error bar-like symbol at TA = -70° shows a possible maximum rotational brightness amplitude. The star symbol shows an upper limiting magnitude from searching the PS1 database for prediscovery images. The gray shading indicates times when C/2014 S3 was not observable because it was in solar conjunction.

The overall shape of the spectrum and, particularly, the 1- μm dip in the spectral reflectivity of C/2014 S3 showed that its surface was consistent with S-type asteroids, typically found in the inner asteroid main belt; the spectrum was inconsistent with all other minor body surfaces: typical comets, trans-Neptunian objects, and asteroids of all other classes. Comets (and trans-Neptunian objects, a reservoir from which a class of comets comes) are believed to have formed in the outer solar system, and their wide range of neutral to red colors reflect a mix of organics, ice, and surface-weathering processes. On the other hand, moderately red S-type bodies are believed to have formed relatively dry in the inner solar system. S-type asteroids, which have been associated with OCs, are generally expected to be dry. Type 4 to type 6 OCs consist of anhydrous minerals, and their mineral assemblages reflect dry thermal metamorphism (15). However, some type 3 OCs have experienced aqueous alteration that has converted matrix minerals and some chondrule glass into hydrous phases (15, 28). The general expectation is that the type 3 OCs come from near the surface of the parent asteroid, where metamorphic temperatures were lowest. It is not clear whether we have samples of the true asteroid surface because that material may not be tough enough to survive passage through space and through the atmosphere to reach Earth; thus, the presence of a tail on object C/2014 S3 and the indication of hydrated silicates in the spectrum were not entirely inconsistent with this object being chondritic.

C/2014 S3 was observed with a dust coma at 2.1 and 2.2 AU (see Fig. 2). By 2.3 AU, the activity had decreased, but a small coma was still visible. To test whether the dust coma was caused by volatile outgassing or by a collision, we constructed a simple water ice sublimation model (see section S4). We did not have enough data to fully constrain an ice sublimation model, but the data were consistent with the behavior expected of dust dragged from the nucleus by sublimating water ice (Fig. 3). We ran two models—one assuming typical icy comet characteristics (albedo of 4%) and one assuming typical S-type reflectivity (25%). The S-type model provided a better match to the data. In both cases, the implied nucleus was small, with a radius between 0.7 and 0.25 km, respectively. The implied gas production rate at perihelion was low, between 3×10^{23} and 1×10^{24} molecules/s, equivalent to a sublimating patch of pure ice 10 to 30 m in radius and five to six orders of magnitude lower than typical Oort cloud comets at the same heliocentric distance.

The appearance of the dust coma was also more consistent with continuous activity than with an impact. The coma extended far outside the syndyne and synchronic envelope, which describes the locus of dust grains of different sizes emitted from the nucleus with zero velocity at different times, accounting for the solar gravity and radiation pressure (see section S5), particularly to the south and to the southwest of the September and October images, respectively (as shown in Fig. 2). This indicates that the dust was ejected with a moderate but nonzero velocity. At the heliocentric distance of C/2014 S3, the grains should be lifted off the surface by a tenuous gas flow with a velocity of 730 m/s (29). Distribution of velocities in amplitude and direction, as expected for a sublimating body, will result in a blurring of the syndyne and synchronic pattern, as observed.

In the region covered by the synchrones and syndynes, the dust extended over a wide range of synchrones, suggesting a wide range of emission times, although the timestamps are approximate because of the initial velocity of the dust. In the competing hypothesis of a high-velocity impact on a small body with weak self-gravitation, ejecta are expected to be launched in a characteristic ejection cone. After some days or weeks, this cone results in a very distinct coma. Such a case was modeled in detail for another body of similar size at similar distance showing a wide range of resulting coma features (30). Whereas the variety of possible collision geometries was enormous, the most salient features in the dust cloud were always parallel to the synchronic corresponding to the time of the impact. This reflected the fact that the impulsive dust emission released a full distribution of dust grain sizes at a single epoch. The fact that the coma of C/2014 S3 did not have any preferential direction indicated that the emission was not impulsive, as it would be in an impact.

We calculated the probability of an impact on C/2014 S3 of a meter-sized (or larger) object on its current orbit while crossing the asteroid belt. This was done considering the number density of meter-sized asteroids in the asteroid belt volume ($3.9 \times 10^{-14} \text{ km}^{-3}$) and the physical radius of C/2014 S3 (0.7 km) and its relative speed while crossing the belt (42 km/s). The probability of a collision before we observed C/2014 S3 was 5×10^{-5} . Thus, it was very unlikely that the dust coma was caused by an impact. Some inner main belt asteroids were suspected to shed dust because they were spun up to their critical rotation periods by radiation pressure effects. This did not apply to C/2014 S3, which spent most of its orbit far from the Sun. Overall, we were therefore confident that the coma was produced by sublimation.

We estimated that, in today's solar system, about 200-km-sized S-type asteroids escaped from the main asteroid belt per million years (31). Approximately 20 of these were scattered by Jupiter, and of these, about one passed through the Oort cloud and could be reinjected inward on a Manx orbit. This would amount to only 0.4 returning objects per million years; thus, it is unlikely that we will observe this contamination. C/2014 S3 is not such an object because it is active, whereas today's S-type asteroids are not. Therefore, we are confident that C/2014 S3 is a rocky planetesimal formed in the inner solar system and ejected to the Oort cloud at the time of planet formation.

SUPPLEMENTARY MATERIALS

Supplementary material for this article is available at <http://advances.sciencemag.org/cgi/content/full/2/4/e1600038/DC1>

- S1. Solar system formation model predictions
- S2. Details of the observations
- S3. Data reduction
- S4. Conceptual ice sublimation model
- S5. Finson-Probst dust models
- S6. Statistical assessment: Manx observations and dynamical models table S1. Observing circumstances.
- References (33–53)

REFERENCES AND NOTES

1. K. J. Walsh, A. Morbidelli, S. N. Raymond, D. P. O'Brien, A. M. Mandell, A low mass for Mars from Jupiter's early gas-driven migration. *Nature* **475**, 206–209 (2011).
2. A. Shannon, A. P. Jackson, D. Veras, M. Wyatt, Eight billion asteroids in the Oort cloud. *Mon. Not. R. Astron. Soc.* **446**, 2059–2064 (2015).
3. P. R. Weissman, H. F. Levison, Origin and evolution of the unusual object 1996 PW: Asteroids from the Oort cloud? *Astrophys. J. Lett.* **488**, L133–L136 (1997).
4. A. Izidoro, K. de Souza Torres, O. C. Winter, N. Haghighipour, A compound model for the origin of Earth's water. *Astrophys. J.* **767**, 54 (2013).
5. H. F. Levison, K. A. Kretke, M. J. Duncan, Growing the gas-giant planets by the gradual accumulation of pebbles. *Nature* **524**, 322–324 (2015).
6. J. H. Oort, The structure of the cloud of comets surrounding the solar system and a hypothesis concerning its origin. *Bull. Astron. Inst. Neth.* **11**, 91–110 (1950).
7. H. F. Levison, A. Morbidelli, L. Dones, R. Jedicke, P. A. Wiegert, W. F. Bottke Jr., The mass disruption of Oort cloud comets. *Science* **296**, 2212–2215 (2002).
8. P. R. Weissman, W. F. Bottke, H. F. Levison, Evolution of comets into asteroids, in *Asteroids III*, W. F. Bottke Jr., A. Cellino, P. Paolicchi, R. P. Binzel, Eds. (University of Arizona Press, Tucson, 2002), pp. 669–686.
9. E. F. Helin, S. Pravdo, K. J. Lawrence, 1996 PW, Minor Planet Electronic Circular 1996-P03, Minor Planet Center, Cambridge, MA (1996).
10. A. J. Brearley, The action of water, in *Meteorites and the Early Solar System II*, D. S. Lauretta, H. Y. McSween, Eds. (University of Arizona Press, Tucson, 2006), pp. 584–624.
11. A. N. Krot, I. D. Hutcheon, A. J. Brearley, O. V. Pravidtseva, M. I. Petaev, C. M. Hohenberg, Timescales and settings for alteration of chondritic meteorites, in *Meteorites and the Early Solar System II*, D. S. Lauretta, H. Y. McSween, Eds. (University of Arizona Press, Tucson, 2006), pp. 525–553.
12. H. H. Hsieh, D. Jewitt, A population of comets in the main asteroid belt. *Science* **312**, 561–563 (2006).
13. M. Küppers, L. O'Rourke, D. Bockelée-Morvan, V. Zakharov, S. Lee, P. von Allmen, B. Carry, D. Teyssier, A. Marston, T. Müller, J. Crovisier, M. Antonietta Barucci, R. Moreno, Localized sources of water vapour on the dwarf planet (1) Ceres. *Nature* **505**, 525–527 (2014).
14. H. Campins, K. Hargrove, N. Pinilla-Alonso, E. S. Howell, M. S. Kelley, J. Licandro, T. Mothé-Diniz, Y. Fernández, J. Ziffer, Water ice and organics on the surface of the asteroid 24 Themis. *Nature* **464**, 1320–1321 (2010).
15. G. R. Huss, A. E. Rubin, J. N. Grossman, Thermal metamorphism in chondrites, in *Meteorites and the Early Solar System II*, D. S. Lauretta, H. Y. McSween Jr., Eds. (University of Arizona Press, Tucson, 2006), pp. 567–586.
16. T. H. Burbine, T. J. McCoy, A. Meibom, B. Gladman, K. Keil, Meteoritic parent bodies: Their number and identification, in *Asteroids III*, W. F. Bottke, A. Cellino, P. Paolicchi, R. P. Binzel, Eds. (University of Arizona Press, Tucson, 2002), pp. 653–667.
17. T. Mikouchi, M. Komatsu, K. Hagiya, K. Ohsumi, M. E. Zolensky, V. Hoffmann, J. Martinez, R. Hochleitner, M. Kaliwoda, Y. Terada, N. Yagi, M. Takata, W. Satake, Y. Aoyagi, A. Takenouchi, Y. Karouji, M. Uesugi, T. Yada, Mineralogy and crystallography of some Itokawa particles returned by the Hayabusa asteroidal sample return mission. *Earth Planets Space* **66**, 82 (2014).
18. T. Nakamura, T. Noguchi, M. Tanaka, M. E. Zolensky, M. Kimura, A. Tsuchiyama, A. Nakato, T. Ogami, H. Ishida, M. Uesugi, T. Yada, K. Shirai, A. Fujimura, R. Okazaki, S. A. Sandford, Y. Ishibashi, M. Abe, T. Okada, M. Ueno, T. Mukai, M. Yoshikawa, J. Kawaguchi, Itokawa dust particles: A direct link between S-type asteroids and ordinary chondrites. *Science* **333**, 1113–1116 (2011).
19. M. J. Gaffey, J. F. Bell, R. H. Brown, T. H. Burbine, J. L. Piatek, K. L. Reed, D. A. Chaky, Mineralogical variations within the S-type asteroid class. *Icarus* **106**, 573–602 (1993).
20. P. Vernazza, B. Zanda, R. P. Binzel, T. Hiroi, F. E. DeMeo, M. Birlan, R. Hewins, L. Ricci, P. Barge, M. Lockhart, Multiple and fast: The accretion of ordinary chondrite parent bodies. *Astrophys. J.* **791**, 120 (2014).
21. P. M. Doyle, K. Jogo, K. Nagashima, A. N. Krot, Early aqueous activity on the ordinary and carbonaceous chondrite parent bodies recorded by fayalite. *Nat. Commun.* **6**, 7444 (2015).
22. A. Rotundi, H. Sierks, V. Della Corte, M. Fulle, P. J. Gutierrez, L. Lara, C. Barbieri, P. L. Lamy, R. Rodrigo, D. Koschny, H. Rickman, H. U. Keller, J. J. López-Moreno, M. Accolla, J. Agarwal, M. F. A'Hearn, N. Altobelli, F. Angrilli, M. A. Barucci, J.-L. Bertaux, I. Bertini, D. Bodewits, E. Bussoletti, L. Colangeli, M. Cosi, G. Cremonese, J.-F. Crifo, V. Da Deppo, B. Davidsson, S. Debei, M. De Cecco, F. Esposito, M. Ferrari, S. Fornasier, F. Giovane, B. Gustafson, S. F. Green, O. Groussin, E. Grün, C. Güttler, M. L. Herranz, S. F. Hviid, W. Ip, S. Ivanovski, J. M. Jerónimo, L. Jorda, J. Knollenberg, R. Kramm, E. Kürt, M. Küppers, M. Lazzarin, M. R. Leese, A. C. López-Jiménez, F. Lucarelli, S. C. Lowry, F. Marzari, E. M. Epifani, J. A. M. McDonnell, V. Mennella, H. Michalik, A. Molina, R. Morales, F. Moreno, S. Mottola, G. Naletto, N. Oklay, J. L. Ortiz, E. Palomba, P. Palumbo, J.-M. Perrin, J. Rodríguez, L. Sabau, C. Snodgrass, R. Sordini, N. Thomas, C. Tubiana, J.-B. Vincent, P. Weissman, K.-P. Wenzel, V. Zakharov, J. C. Zarnecki, Dust measurements in the coma of comet 67P/Churyumov-Gerasimenko inbound to the Sun. *Science* **347**, aaa3905 (2015).
23. K. Baillié, S. Charnoz, E. Pantin, Time evolution of snow regions and planet traps in an evolving protoplanetary disk. *Astron. Astrophys.* **577**, A65 (2015).
24. M. E. Zolensky, T. J. Zega, H. Yano, S. Wirick, A. Westphal, M. K. Weisberg, I. Weber, J. L. Warren, M. A. Velbel, A. Tsuchiyama, P. Tsou, A. Toppani, N. Tomioka, K. Tomeoka, N. Teslich, M. Taheri, J. Susini, R. Stroud, T. Stephan, F. J. Stadermann, C. J. Snead, S. B. Simon, A. Simionovici, T. H. See, F. Robert, F. J. M. Rietmeijer, W. Rao, M. C. Perronnet, D. A. Papanastassiou, K. Okudaira, K. Ohsumi, I. Ohnishi, K. Nakamura-Messenger, T. Nakamura, S. Mostefaoui, T. Mikouchi, A. Meibom, G. Matrajt, M. A. Marcus, H. Leroux, L. Lemelle, L. Le, A. Lanzirotti, F. Langenhorst, A. N. Krot, L. P. Keller, A. T. Kearsley, D. Joswiak, D. Jacob, H. Ishii, R. Harvey, K. Hagiya, L. Grossman, J. N. Grossman, G. A. Graham, M. Gounelle, P. Gillet, M. J. Genge, G. Flynn, T. Ferroir, S. Fallon, D. S. Ebel, Z. R. Dai, P. Cordier, B. Clark, M. Chi, A. L. Butterworth, D. E. Brownlee, J. C. Bridges, S. Brennan, A. Brearley, J. P. Bradley, P. Bleuet, P. A. Bland, R. Bastien, Mineralogy and petrology of Comet 81P/Wild 2 nucleus samples. *Science* **314**, 1735–1739 (2006).
25. M. E. Zolensky, R. J. Bodnar, E. K. Gibson Jr., L. E. Nyquist, Y. Reese, C.-Y. Shih, H. Wiesmann, Asteroidal water within fluid inclusion-bearing halite in an H5 chondrite, Monahans (1998). *Science* **285**, 1377–1379 (1999).
26. M. Gounelle, M. E. Zolensky, The Orgueil meteorite: 150 years of history. *Meteorit. Planet. Sci.* **49**, 1769–1794 (2014).
27. L. Dones, R. Brasser, N. Kaib, H. Rickman, Origin and evolution of the cometary reservoirs. *Space Sci. Rev.* **197**, 191–269 (2015).
28. M. K. Weisberg, T. J. McCoy, A. N. Krot, Systematics and evaluation of meteorite classification, in *Meteorites and the Early Solar System II*, D. S. Lauretta, H. Y. McSween Jr., Eds. (University of Arizona Press, Tucson, 2006), pp. 19–52.
29. N. T. Bobrovnikoff, Physical properties of comets. *Astron. J.* **59**, 357–358 (1954).
30. J. Kleyna, O. R. Hainaut, K. J. Meech, P/2010 A2 LINEAR. II. Dynamical dust modelling. *Astron. Astrophys.* **549**, A13 (2013).
31. W. F. Bottke Jr., A. Morbidelli, R. Jedicke, J.-M. Petit, H. F. Levison, P. Michel, T. S. Metcalfe, Debaised orbital and absolute magnitude distribution of the near-Earth objects. *Icarus* **156**, 399–433 (2002).
32. S. J. Bus, R. P. Binzel, Phase II of the small main-belt asteroid spectroscopic survey: The observations. *Icarus* **158**, 106–145 (2002).
33. F. Masset, M. Snellgrove, Reversing type II migration: Resonance trapping of a lighter giant protoplanet. *Mon. Not. R. Astron. Soc.* **320**, L55–L59 (2001).
34. K. Tsiganis, R. Gomes, A. Morbidelli, H. F. Levison, Origin of the orbital architecture of the giant planets of the solar system. *Nature* **435**, 459–461 (2005).
35. R. Brasser, A. Morbidelli, Oort Cloud and scattered disc formation during a late dynamical instability in the solar system, *Asteroids, Comets, Meteors 2012 (LPI Contribution No. 1667, id.6005), Proceedings of the Conference, Niigata, Japan, 16–20 May 2012*.
36. R. Brasser, M. J. Duncan, H. F. Levison, Embedded star clusters and the formation of the Oort Cloud. *Icarus* **184**, 59–82 (2006).
37. R. Brasser, M. E. Schwamb, Re-assessing the formation of the inner Oort cloud in an embedded star cluster—II. Probing the inner edge. *Mon. Not. R. Astron. Soc.* **446**, 3788–3796 (2015).

38. C. Hayashi, Structure of the solar nebula, growth and decay of magnetic fields and effects of magnetic and turbulent viscosities on the nebula. *Prog. Theor. Phys. Suppl.* **70**, 35–53 (1981).
39. R. J. Walker, Highly siderophile elements in the Earth, Moon and Mars: Update and implications for planetary accretion and differentiation. *Chem. Erde Geochem.* **69**, 101–125 (2009).
40. L. Dones, P. R. Weissman, H. F. Levison, M. J. Duncan, Oort cloud formation and dynamics, in *Comets II*, M. C. Festou, H. U. Keller, H. A. Weaver, Eds. (University of Arizona Press, Tucson, 2004), pp. 153–174.
41. M. Lambrechts, A. Johansen, Rapid growth of gas-giant cores by pebble accretion. *Astron. Astrophys.* **544**, A32 (2012).
42. B. M. S. Hansen, Formation of the terrestrial planets from a narrow annulus. *Astrophys. J.* **703**, 1131–1140 (2009).
43. M. Fukugita, T. Ichikawa, J. E. Gunn, M. Doi, K. Shimasaku, D. P. Schneider, The Sloan digital sky survey photometric system. *Astron. J.* **111**, 1748–1756 (1996).
44. E. A. Magnier, E. Schlafly, D. Finkbeiner, M. Juric, J. L. Tonry, W. S. Burgett, K. C. Chambers, H. A. Flewelling, N. Kaiser, R.-P. Kudritzki, J. S. Morgan, P. A. Price, W. E. Sweeney, C. W. Stubbs, The Pan-STARRS 1 photometric reference ladder, release 12.01. *Astrophys. J. Suppl. Ser.* **205**, 20 (2013).
45. J. L. Tonry, C. W. Stubbs, K. R. Lykke, P. Doherty, I. S. Shivvers, W. S. Burgett, K. C. Chambers, K. W. Hodapp, N. Kaiser, R.-P. Kudritzki, E. A. Magnier, J. S. Morgan, P. A. Price, R. J. Wainscoat, The Pan-STARRS 1 photometric system. *Astrophys. J.* **750**, 14 (2012).
46. E. Bertin, S. Arnouts, SExtractor: Software for source extraction. *Astron. Astrophys. Suppl. Ser.* **117**, 393–404 (1996).
47. K. J. Meech, D. Jewitt, G. R. Ricker, Early photometry of comet P/Halley: Development of the coma. *Icarus* **66**, 561–574 (1986).
48. C. Snodgrass, C. Tubiana, D. M. Bramich, K. Meech, H. Boehnhardt, L. Barrera, Beginning of activity in 67P/Churyumov-Gerasimenko and predictions for 2014–2015. *Astron. Astrophys.* **557**, A33 (2013).
49. N. Fray, B. Schmitt, Sublimation of ices of astrophysical interest: A bibliographic review. *Planet Space Sci.* **57**, 2053–2080 (2009).
50. O. Groussin, J. M. Sunshine, L. M. Feaga, L. Jorda, P. C. Thomas, J.-Y. Li, M. F. A'Hearn, M. J. S. Belton, S. Besse, B. Carcich, T. L. Farnham, D. Hampton, K. Klaasen, C. Lisse, F. Merlin, S. Protopapa, The temperature, thermal inertia, roughness and color of the nuclei of Comets 103P/Hartley 2 and 9P/Tempel 1. *Icarus* **222**, 580–594 (2013).
51. M. J. Finson, R. F. Probstein, A theory of dust comets. I. Model and equations. *Astrophys. J.* **154**, 327–352 (1968).
52. D. T. Britt, D. Yeomans, K. Housen, G. Consolmagno, Asteroid density, porosity, and structure, in *Asteroids III*, W. F. Bottke Jr., A. Cellino, P. Paolicchi, R. P. Binzel, Eds. (University of Arizona Press, Tucson, 2002), pp. 485–500.
53. P. Wiegert, S. Tremaine, The evolution of long-period comets. *Icarus* **137**, 84–121 (1999).

Acknowledgments: This study was based on observations obtained with MegaPrime/MegaCam, a joint project of CFHT and CEA/DAPNIA, at the CFHT, which is operated by the National Research Council (NRC) of Canada, the Institut National des Sciences de l'Univers of the Centre National de la Recherche Scientifique of France, and the University of Hawaii (programs 14bh07 and 14bh27) and the European Organisation for Astronomical Research in the Southern Hemisphere under ESO program 294.C-5009(A). Given that the comet was rapidly fading, we are grateful to the ESO Director General for swiftly approving our DDT (Director's Discretionary Time) request (within 5 hours of receipt of the proposal). It was this rapid turnaround that made this observation possible. We also thank the exceptional VLT UT1 science operations staff and F. Patat, who managed to get the program into the queue within 48 hours of proposal submission. We also thank G. Huss for useful discussions. **Funding:** K.J.M., J.V.K., and J.K. acknowledge support through the NASA Astrobiology Institute and partial support through NASA grant NNX13A151G and NSF grant AST1413736. S.B. acknowledges support through the European Research Council Advanced Grant HotMol ERC-2011-AdG-291659, and R.J.W. acknowledges support by NASA under grants NNX12AR65G and NNX14AM74G. A.M. acknowledges support by the French Agence Nationale de la Recherche project number ANR-13-13-BS05-0003-01, project MOJO (Modeling the Origin of Jovian planets). **Author contributions:** K.J.M. conceived of the project, secured the telescope time, and developed the sublimation models. R.J.W. alerted the team to the PS1 discovery and obtained some of the imaging observations. M.M. performed the astrometry and searched for additional images in the PS1 database. O.R.H. prepared the observations for the VLT, and B.Y. carried out the observations. B.Y., S.B., and O.R.H. performed the spectral reductions. J.K. prepared the imaging observations and performed the photometric reductions. J.V.K. contributed to the analysis and interpretation of the data. A.M. provided the dynamical discussion and calculated the impact probabilities. **Competing interests:** The authors declare that they have no competing interests. **Data and materials availability:** All data needed to evaluate the conclusions in the paper are present in the paper, in the Supplementary Materials, and/or through the following data archives: (i) the VLT data are accessible through the ESO Science Archive Facility at <http://archive.eso.org/cms.html>; and (ii) the CFHT data are accessible through the Canadian Astronomy Data Centre at www.cadc-ccda.hia-ihc.nrc-cnrc.gc.ca/en/.

Submitted 8 January 2016

Accepted 30 March 2016

Published 29 April 2016

10.1126/sciadv.1600038

Citation: K. J. Meech, B. Yang, J. Kleyna, O. R. Hainaut, S. Berdyugina, J. V. Keane, M. Micheli, A. Morbidelli, R. J. Wainscoat, Inner solar system material discovered in the Oort cloud. *Sci. Adv.* **2**, e1600038 (2016).

Inner solar system material discovered in the Oort cloud

Karen J. Meech, Bin Yang, Jan Kleyna, Olivier R. Hainaut, Svetlana Berdyugina, Jacqueline V. Keane, Marco Micheli, Alessandro Morbidelli and Richard J. Wainscoat

Sci Adv 2 (4), e1600038.
DOI: 10.1126/sciadv.1600038

ARTICLE TOOLS	http://advances.sciencemag.org/content/2/4/e1600038
SUPPLEMENTARY MATERIALS	http://advances.sciencemag.org/content/suppl/2016/04/26/2.4.e1600038.DC1
REFERENCES	This article cites 43 articles, 6 of which you can access for free http://advances.sciencemag.org/content/2/4/e1600038#BIBL
PERMISSIONS	http://www.sciencemag.org/help/reprints-and-permissions

Use of this article is subject to the [Terms of Service](#)

Science Advances (ISSN 2375-2548) is published by the American Association for the Advancement of Science, 1200 New York Avenue NW, Washington, DC 20005. The title *Science Advances* is a registered trademark of AAAS.

Copyright © 2016, The Authors